Visualization and Quantification of the Mechanical Deformation Induced by an Electrical Field in Poly(ethylene naphthalene 2,6-dicarboxylate) (PEN) Films

Boubakeur Zegnini,* Nadine Lahoud, Laurent Boudou, Juan Martinez-Vega

Laboratoire Plasma et Conversion d'Energie (UMR-CNRS 5213), University of Toulouse, 118 route de Narbonne, 31062 Toulouse cedex, France

Received 17 May 2007; accepted 18 March 2008
DOI 10.1002/app.28434
Published online 11 June 2008 in Wiley InterScience (www.interscience.wiley.com).

ABSTRACT: An optical nondestructive strain measurement technique was performed to analyze the mechanical deformation induced by an electrical field within the insulating materials. Poly(ethylene naphthalene 2,6-dicarboxylate) (PEN) films were then subjected to constant electrical fields right up to their electrical breakdown. The experimental technique made it possible to follow the various stages of the mechanical behavior of PEN in real time. The final breakdown occurred in the observation zone and the related mechanical deformation was captured. A "margarita" structure was observed with a hole at the center. The experimental results indicated that the level of the induced-mechanical deformations depended on the local environment. We defined two different zones representing the inside and the outside of the damaged area. The induced-deformations were larger in the damaged zone. It was also observed that deformations increased when the sample had a lower degree of crystallinity. © 2008 Wiley Periodicals, Inc. J Appl Polym Sci 110: 23–29, 2008

Key words: ageing; dielectric properties; crystallization; damage zone; microdeformation

INTRODUCTION

Poly(ethylene naphthalene 2,6-dicarboxylate) (PEN) is a thermoplastic polyester synthesized by polycondensation of 2,6-naphtalenedicarboxylic acid and ethylene glycol[1–3] and have the chemical structure as shown in Figure 1.

The rigid naphthalene ring in the repeat unit of PEN provides a higher stiffness to the macromolecular chain and hence yields better thermal, mechanical, and dielectric properties compared with poly(ethylene terephthalate) (PET)[4–6] which has only a *para*-substituted phenyl group in the backbone. Thanks to these improved properties; PEN became a strong candidate for the very demanding requirements of electrical engineering like the thermal stress in surface-mounted technology, the demand for a longer lifetime of electrical devices and finally, the miniaturization of capacitors.[7] As a consequence, these applications require a wider investigation of the material responses under high electrical fields. Indeed, this subject gained a lot of ground in the literature.[8–11] The aim of our work is a better understanding of the mechanical influence of electrical stresses on solid insulating materials. It has been established, experimentally, that these induced mechanical stresses are responsible for highly localized mechanical deformation in some polymer films and thus have an important participation in the ageing process of organic insulators. The mechanical response of PEN films is described in terms of induced-mechanical deformations depending on several parameters as will be shown in the following article.

To carry out this work, we used an "optical noncontact strain measurement technique" developed by Dupré and coworkers.[12,13] This method makes it possible to follow in real time the various stages of the mechanical behavior of PEN films during the application of a DC electrical field. We compared the evolution of the field-induced deformation in amorphous and partially crystallized PEN samples. The level of deformation has been measured as a function of electrical field at two different degrees of crystallinity.

EXPERIMENTAL

Materials and morphological characterization

Commercial PEN (Teonex TM) provided by DuPont Teijin Films (Luxembourg) was studied. The samples were obtained as amorphous films with thicknesses

**Permanent address:* Laboratoire d'Etudes et de Développement des Matériaux Semi-Conducteurs et Diélectriques, University of Laghouat, BP 37 G, route de Ghardaïa, Laghouat 03000, Algeria.

Correspondence to: J. Martinez-Vega (juan.martinez@laplace.univ-tlse.fr).

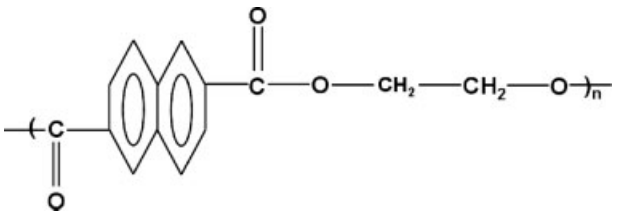

Figure 1 Chemical formula of PEN.

TABLE I
Main Characteristics of the Provided PEN Films

Micro morphology	Amorphous
Density	1.38 g/cm^3
Young modulus at room temperature	6.08 GPa
Tensile strength at room temperature	275 MPa
Resistivity	10^{18} Ω cm
Breakdown voltage	300 kV/mm

of 25 and 70 μm. The main characteristics of these materials are reported in Table I.

Semicrystalline samples were obtained by annealing the "as received" amorphous PEN at 170°C. Different annealing durations were undertaken to obtain PEN samples with different degrees of crystallinity.

To determine the morphology of the samples, we used the differential scanning calorimetry (DSC) technique. The measurements were carried out using a 2010 TA instrument between 30 and 300°C, the heating rate being 10°C/min. The sample weights were ~12 mg. The initial amorphous PEN samples were first maintained at an annealing temperature of 170°C for 5, 10, 15, 30, 45, 60, 90, 120, and 180 min. They were then cooled down to 30°C with a cooling rate of 10°C/min. The physical phenomena associated with the various phase transitions during the endothermic and exothermic processes presented on the DCS thermogram were thus detected and quantified. Crystallization and melting temperatures were deduced from the locations of the peak-maximums. The degrees of crystallinity were calculated from the melting enthalpy using the value of 103.4 J/g corresponding to a 100% crystalline PEN.[14]

Samples to be tested were metallized; a gold layer was deposited on the surface under vacuum with an S150B sputter coater. Two metallized areas, 20 mm in diameter and 30-nm thick, were thus obtained on the two faces of a film; this made it possible to guarantee a better electrode/polymer contact and also obtain a reflective surface. To eliminate the initial charges existing on the faces, we short-circuited each test sample for a few hours before the testing.

DSC measurements were also carried out on the metallized samples. The corresponding thermograms show, practically, no differences between initial and metallized samples indicating no appreciable effect of gold metallization on the morphological properties of the PEN films in this case.

Experimental device

As previously mentioned, an optical technique was used to follow-up and quantify in real time the mechanical deformation induced by a DC electrical field on PEN thin films. This technique has been set up as an experimental device by Mamy and coworkers,[9] and is schematically represented in Figure 2.

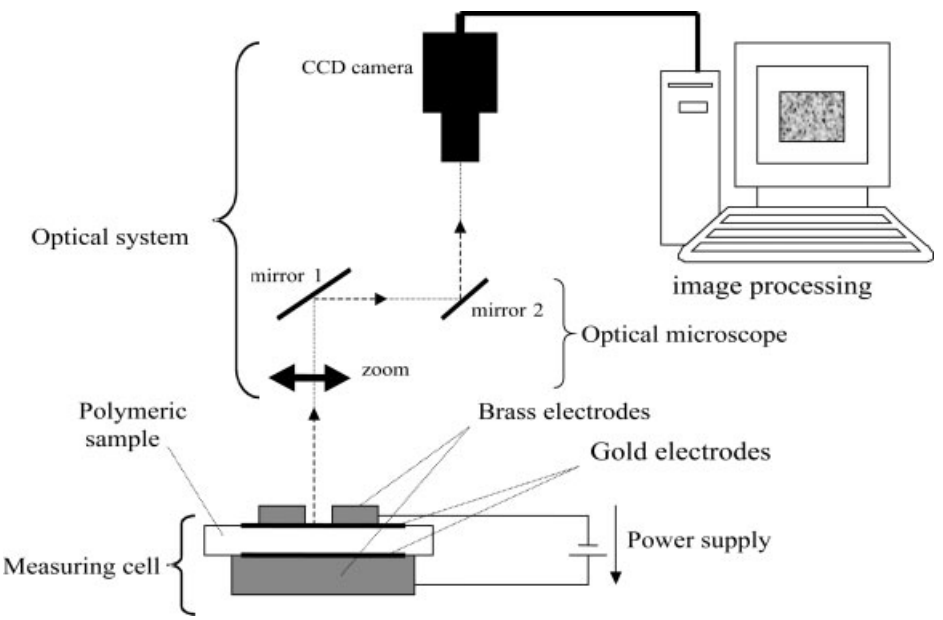

Figure 2 The experimental set-up.

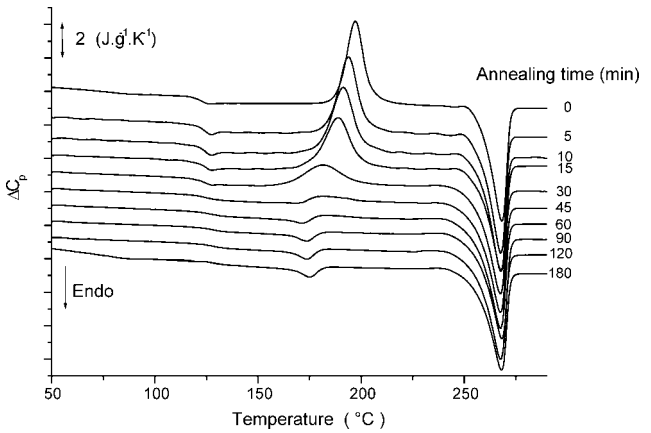

Figure 3 DSC thermograms of the PEN amorphous (without annealing) and semicrystalline (5–180 min of annealing) samples.

It included three essential parts: a sample-holder cell which contained the sample to be tested and two brass electrodes. The upper electrode of the cell was pierced with a 12-mm-diameter hole, which allowed the observation of the surface. The entire system was fed by a direct-current high-voltage source (HCN 35-20000) that delivered a maximum voltage of 20 kV and a current limited to 1.5 mA. An optical system, which included an optical microscope connected to a charge-coupled device (CDD) camera (resolution = 768 pixels × 576 pixels with 256 gray levels), permitted the observation of the sample surface in reflected light. A data-processing unit, the DEFTAC V2005 software associated with the image processing system MATROX METEOR II, permitted to keep control over the experiment.[15,16]

Measurements were carried out under room conditions and for short durations to minimize the influence of the environment. This technique is based on the tracking of four markers, forming a cross, present on the surface of a gold metallized sample. When a gradually increasing step voltage is applied to the sample, the markers move, and a computerized tracking of the successive positions of the four markers permit us to quantify the induced deformation using Lagrangean formalism as described in details in Refs. 9, 15, and 17. The experimental technique makes it possible to measure five induced-mechanical deformation components associated with the film plane surface. These components are labeled as ε_x, ε_y, and γ_{xy}, which are associated with the directions parallel to the x-, y-, and xy-shearing axes, respectively. The ε_1 and ε_2 components are associated with the principal directions at which, γ_{xy} is nil. We have assumed the homogeneity of the deformation on the measurement base, and as a result, the reported values are average ones.[9]

RESULTS AND DISCUSSION

DSC measurements

Typical calorimetry results are displayed in Figure 3 for the initially amorphous and the thermally crystallized (at 170°C) PEN films. The semicrystalline films were obtained with different annealing times (5, 10, 15, 30, 45, 60, 90, 120, and 180 min).

The thermogram shows the glass transition temperature (T_g) at 123°C for the amorphous sample. For other samples, the glass transition temperature T_g shifts towards higher temperatures and becomes less pronounced when the annealing time increases. This shift towards higher temperatures happens because the mobility of the chain segments, which is necessary to promote the recovery enthalpy, decreases during the crystallization process.[18] The peak-magnitude is an indirect measure of the enthalpy relaxation during the annealing process.

As the temperature increases, the cold crystallization and the melting point of PEN can be observed successively. The cold crystallization peak significantly decreases when the annealing time increases as shown in Figure 3. Above 45 min of annealing duration, this peak is almost the same for different samples. In fact, the cold crystallization process is known to be originating from the rearrangement of amorphous regions into crystalline phases while heating and then it is directly related to the presence of amorphous phases. As expected, at higher temperatures, the melting peak of PEN does not seem to be affected by the duration of the isothermal annealing treatment.

The degree of crystallinity χ was calculated for the different PEN samples over different annealing times. The results are shown in Figure 4.

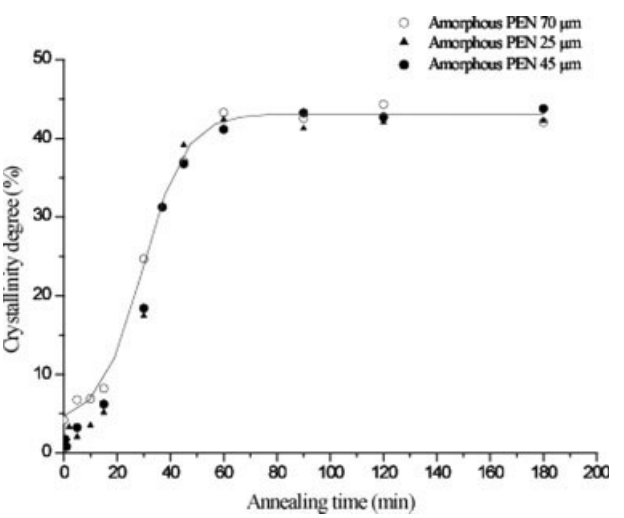

Figure 4 Crystallinity percentage of PEN films as a function of their annealing time.

A sigmoid evolution of the degree of crystallinity as a function of the annealing time occurred. The evolution is observed in three steps, the first one corresponds to annealing times smaller than 15 min, when the material remains almost amorphous. Subsequently, a fast crystallization rate is observed, between 15 and 45 min attaining 45% of crystallinity percentage. This value remains constant over longer periods of annealing. This phenomenon is probably due to the elimination of voids present in the material and involves slight lamellar thickening and crystallization to form extended chain regions.[19] In other words, during this phase the degree of crystallinity does not change but crystallites with better organized structure are formed. The values of crystallinity ratios for different annealing times are in good agreement with the heat flow profiles presented in Figure 3.

Mechanically-induced deformation measurements

An optical observation of the PEN thin film surface was undertaken to analyze the induced mechanical deformation under a high electrical field. PEN films were subjected to a gradual direct-current voltage increase in 0.5 kV steps. The application time of a voltage step was fixed at 200 s. The film deformation was recorded with the CDD camera with a sample imaging rate of one image per two and a half seconds.

Using this device, we obtained an image of the gold-metallized surface of a PEN sample. Figure 5 shows the initial image (electrical field = 0) of a partially crystallized PEN annealed at 170°C during 30 min with a crystallinity degree of 17.42%. The image reveals small, contrasting spots which represent the microscopic light-contrast of a traditional metallization. To manipulate the test sample as little as possible, we identified four of these spots with computerized marking. The four markers thus obtained allowed us to quantify the mechanical deformation induced in real time by the applied electrical field.

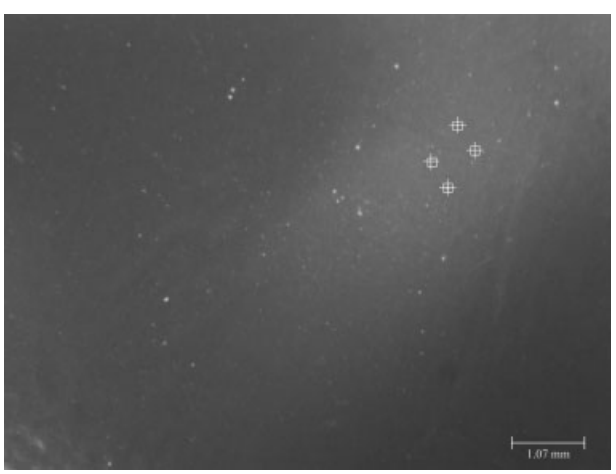

Figure 5 The initial image of a gold-metallized partially crystallized PEN with χ = 17.42%. Identification of four spots with an average marker distance of 0.6 mm.

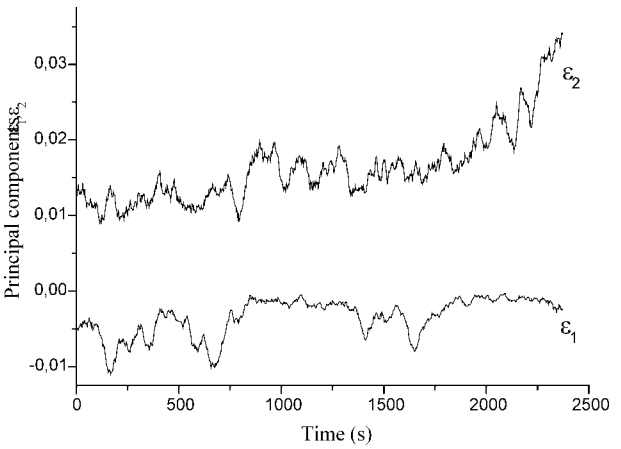

Figure 6 Evolution of principal strain components under an applied electrical field for the PEN film (χ = 17.42%).

Under an applied electrical field, an induced-mechanical deformation occurred in the sample. Figure 6 shows the evolution of the principal induced-deformation components, ε_1 and ε_2, of the PEN film (χ = 17.42%) until the final electrical breakdown. It is interesting to note that ε_1 is positive and ε_2 is negative (even though it is close to zero). This anisotropy is probably due to the biaxial orientation of the film micromorphology during the manufacturing process.

In Figure 7, we reported the total mechanical deformation or equivalent strain[20] as a function of the electrical field, until the electrical breakdown. This parameter is calculated with the average fitted values of ε_1 and ε_2.[9] We can notice that the evolution of

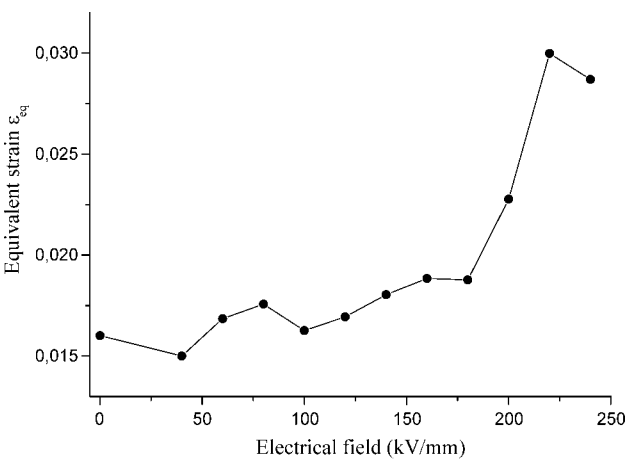

Figure 7 Equivalent strain representation as a function of the applied electrical field until the final electrical breakdown.

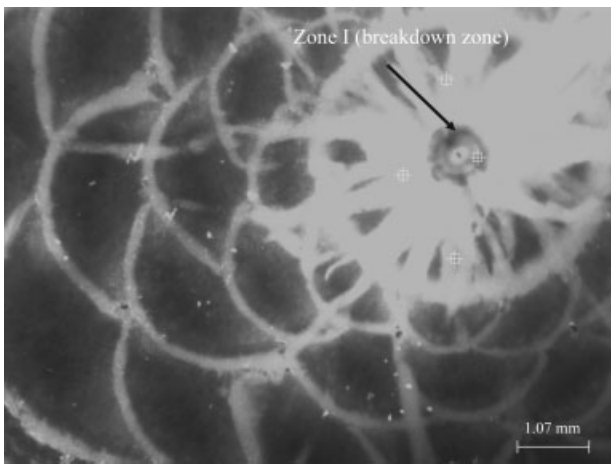

Figure 8 Image of the breakdown zone obtained by the optical surface observation technique.

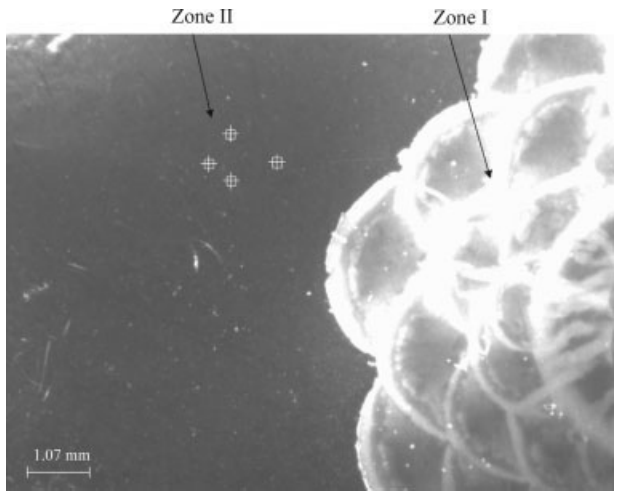

Figure 9 The definition of two different zones of the sample, Zone I inside the breakdown area and Zone II beyond it.

the induced-deformation with the electrical field shows three principal zones: the total deformation is relatively small at fields in the range of 0–175 kV/mm. Above 175 kV/mm, it quickly increases with the electrical field. This field value forms the definition of a threshold field, that is, the electrical field beyond which the deformation progresses quickly as an avalanche process. Finally, the decrease of the equivalent strain before the electrical breakdown could be explained by a flow of the material placed between the electrodes or by a local densification of the material before breakdown.

The particularity of our study is that we observed exactly the zone where the breakdown occurred on the PEN film surface under an applied electrical field. This observation made it possible to visualize and quantify the induced-deformation inside the breakdown zone and to compare it with the deformation outside this zone. By using the optical surface observation technique, the breakdown zone has been clearly identified as shown in Figure 8 (Zone I).

A "margarita" structure was formed on the surface of the metallized sample in the damaged zone (zone I). At the center of this area, a micro hole of 58.6 μm in diameter was produced. A small depressed area of about 0.6 mm was formed around the hole. Radiant microsparks were observed between the center and a ring-shaped corona of about 2.40 mm in diameter. A series of almost circular coronas were formed successively in the surrounding area. These circular coronas are centered at the intersection of previous ones. The radii of the coronas are larger when they are situated away from the center of this structure, having an average value of 750 μm.

By using scanning electron microscopy analysis, superficial damage was also observed. It was interesting to notice that the damage occurred only at the surface exposed to the air; the other side in direct contact with the high voltage electrode remained undamaged.

Our technique allows us to analyze several zones by using same images, which means under exactly the same conditions. In this experiment we chose to analyze two different zones, as shown in Figure 9, to evaluate the induced-deformations occurring inside the damaged area (Zone I) and outside this area (Zone II).

Figure 10 shows the evolution of the induced-deformation in each zone. Zone I shows a larger strain level than Zone II, even at small values of the applied field. This observation relates, in a straightforward way, the locally induced strain to the breakdown phenomenon. Several studies and models have highlighted the role of microdomains in the ageing mechanism and dielectric breakdown of insulating materials.[21–23] A new model describing the

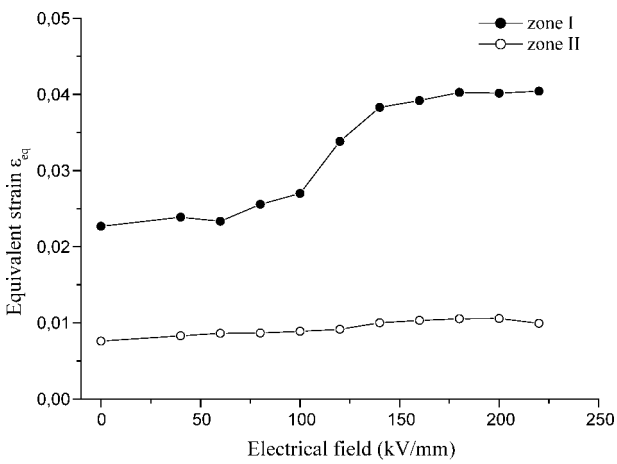

Figure 10 Comparison of the induced deformation levels in each predefined zone.

ageing process in organic insulators and accounting for the multiplicity of local zone strengths inside the material has been elaborated by our research team.[24] The existence of stronger or weaker zones could be explained by the preexistence of defects inside the material or by a localized ageing within a localized zone.

Influence of crystallinity

Two different samples with different degrees of crystallinity were chosen to evaluate the influence of the degree of crystallinity on the induced-deformation level. The previous sample with χ = 17.42%, and another one with χ = 5.14%.

Figures 11 and 12 show the influence of the polymer crystallinity on the strain evolution, and consequently on the electrical breakdown field, in Zone I (damaged zone) and Zone II (outside the damaged zone), respectively. It was observed that the sample with lower crystallinity (χ = 5.14%) presented a larger induced-strain at both Zones I and II. The induced-deformation starts to increase at a lower field for the lower crystalline film. Zone II showed no damage for the 17.42% crystallized sample as already shown. However, the 5.14% crystallized film showed an increase of the induced-deformation level even in the outside damage zone (Fig. 12). These results allow us to confirm that amorphous and crystalline phases in a polymer material do not react in the same way under the application of an electrical field. Indeed, strong intramolecular covalent bonds determine the characteristic of the crystalline lamellae. Intermolecular secondary bonds which exist between the chains in the lamellae and dominate the amorphous interlamellae spaces are much weaker. Paths within the amorphous phase will have relatively low mechanical strength and ductile characteristics.[21]

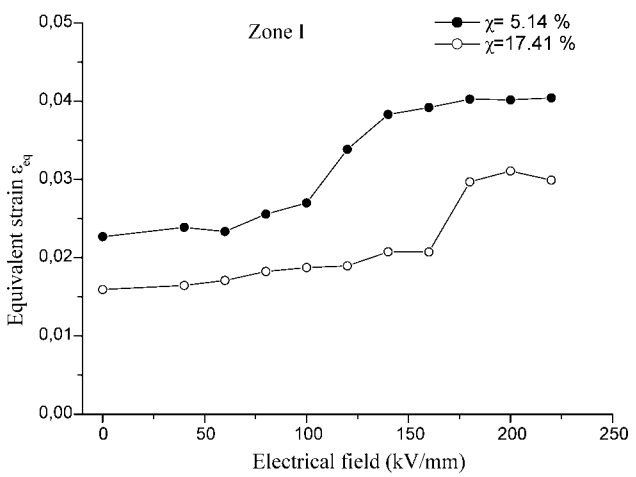

Figure 11 Variation of the induced deformation behavior with the crystallinity degree: Zone I.

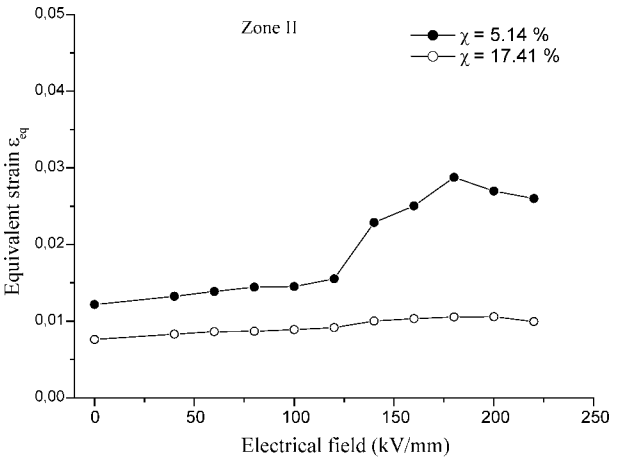

Figure 12 Variation of the induced deformation behavior with the crystallinity degree: Zone II.

These observations allowed us to visualize and better understand the complex nature of polymers. These materials present a large distribution of local environments within the sample, each with different characteristics. This specific property of polymers could be integrated into the methodology of the comprehension of the ageing process occurring inside these materials.

CONCLUSIONS

In this study, we highlighted the mechanical response of PEN films under gradually increasing electrical fields through the quantification of the induced-mechanical deformations. This study was carried out with an optical technique that did not involve any physical contact and was based on the follow-up of four markers on the PEN film surface.

During the application of the electrical field, we were able to film the area where the electrical breakdown occurred. We compared the evolution of the induced-deformation strain inside and outside the damaged area. We noticed that the level of the induced-deformation depended on the structure of the material. We can associate different zones with different dielelectric strengths. Moreover, a study of the mechanical deformation for PEN samples with different degrees of crystallinity indicates a larger deformation in samples with lower crystallinity.

This study allowed us to examine the mechanical response of insulating materials under an electrical field, and it constitutes an important base for the study of the behavior of these solid materials operating under electrical fields or multistress conditions, i.e., involving several stresses. These bases may be very helpful for the comprehension of the ageing process in organic insulators.

We would like to thank DuPont Teijin Films (Luxembourg) for providing us with PEN amorphous samples. The authors thank C. Mayoux (University of Toulouse, France) for helpful discussions.

References

1. Teijin Ltd. Netherlands Patent 72-16920, 1972.
2. Cakmak, M.; Wang, Y. D.; Simhambhatla, M. Polym Eng Sci 1990, 30, 721.
3. Wang, C. S.; Sun, Y. M. J Polym Sci Part A: Polym Chem 1994, 32, 1295.
4. Tonelli, A. E. Polymer 2002, 43, 637.
5. Ghahem, A. M.; Porter, R. S. J Polym Sci Part B: Polym Phys 1989, 27, 480.
6. Santa Cruz, C.; Balta, F. J.; Calleja Zachmann, H. G.; Chen, D. J Mater Sci 1992, 27, 2161.
7. Guastavino, J.; Krauzes, E.; Mayoux, C. IEEE Trans Dielec Elec Insul 1999, 6, 792.
8. Blok, J.; Le Grand, D. G. J Appl Phys 1969, 40, 288.
9. Mamy, P. R.; Martinez-Vega, J.; Duprè, J. C.; Bretagne, N. J Appl Polym Sci 2004, 93, 2313.
10. Jones, J. P.; Lewis, T. J.; Llewellyn, J. P. Proc ICSD 2004 IEEE Inter Conf Sol Dielect, Toulouse, France 2004; Vol. 1, p 284.
11. Connor, P. Conf Elect Insul Dielect Phen 1998, 1, 27.
12. Brèmand, F.; Dupré, J. C.; Lagarde, L. Eur J Mech A/Solid 1992, 11, 349.
13. Brèmand, F.; Dupré, J. C.; Lagarde, L. Photomécanique 1995, 95, 171.
14. Cheng, S. Z.; Wunderlich, B. Maromolecules 1988, 21, 789.
15. Dupré, J. C.; Valle, V.; Brèmand, F. DEFTAC Software Guideline; Laboratoire de Mécanique des Solides, University of Poitiers: France, 2005.
16. Zegnini, B.; Boudou, L.; Martinez-Vega, J.; Macro 2006—41st Int Symp Marcomol Proc, Rio De Janeiro, Brasil, 2006.
17. Bretagne, N.; Dupré, JC. XV^{ème} Cong Fran Méca, Nancy, France, 2001.
18. Alves, N. M.; Mano, J. F.; Balaguer, E.; Meseguer Duenas, J. M.; Gomez Ribelles, J. L. Polymer 2002, 43, 4111.
19. Takenaga, M.; Yamagata, K. J Polym Sci: Polym Phys Ed 2003, 23, 149.
20. Ford. Advanced Mechanics of Materials; Longmans: London, 1963.
21. Jones, J. P.; Llewellyn, J. P.; Lewis, T. J. IEEE Trans Dielect Elect Insul 2005, 12, 951.
22. Crine, J. P. IEEE Trans Dielect Elect Insul 2005, 12, 1089.
23. Mazzanti, G.; Montanari, G. C.; Dissado, L. A. IEEE Trans Dielect Elect Insul 2005, 12, 877.
24. Martinez-Vega, J. Matériaux Diélectriques pour le Génie Electrique—Propriétés, vieillissement et modélisation; Hermès: Lavoisier, 2007; Vol. 1, Chapter 9.